

SMAR: Soft Modality-Aware Routing Strategy for MoE-based Multimodal Large Language Models Preserving Language Capabilities

Guoyang Xia^{1,2}, Yifeng Ding², Fengfa Li², Lei Ren²,
Chen Wei², Fangxiang Feng¹, Xiaojie Wang¹,

¹Beijing University of Posts and Telecommunications, ²Li Auto,

Abstract

Mixture-of-Experts (MoE) architectures have become a key approach for scaling large language models, with growing interest in extending them to multimodal tasks. Existing methods to build multimodal MoE models either incur high training costs or suffer from degraded language capabilities when adapting pretrained models. To address this, we propose Soft Modality-Aware Routing (SMAR), a novel regularization technique that uses Kullback–Leibler divergence to control routing probability distributions across modalities, encouraging expert specialization without modifying model architecture or heavily relying on textual data. Experiments on visual instruction tuning show that SMAR preserves language ability at 86.6% retention with only 2.5% pure text, outperforming baselines while maintaining strong multimodal performance. Our approach offers a practical and efficient solution to balance modality differentiation and language capabilities in multimodal MoE models.

1 Introduction

The Mixture-of-Experts (MoE) architecture has seen increasingly widespread adoption in large language models (LLMs). Models such as Mixtral 8×7B (Jiang et al., 2024) and Deepseek-V3 (Liu et al., 2024) employ sparse MoE structures to achieve a favorable balance between substantially increased parameter capacity and inference efficiency. This architectural approach has demonstrated superior overall performance and has progressively emerged as the dominant design for LLMs in industrial applications. Therefore, in contemporary multimodal large language models (MLLMs), integrating the MoE architecture which supports substantial parameter scaling while maintaining inference efficiency has become a competitive choice for achieving a higher performance upper bound.

Researchers have primarily adopted three approaches to developing MLLMs based on the MoE architecture. The first approach (Li et al., 2024) involves training a MLLM with a MoE architecture from scratch using extensive datasets. However, this training paradigm demands significant computational overhead, constraining both its scalability and broader applicability. The second approach (Lin et al., 2024; Li et al., 2025) involves extending existing dense LLMs into a MoE architecture during multimodal fine-tuning to form multiple experts. However, this strategy frequently results in weak expert specialization due to high parameter redundancy among experts (Huang et al., 2025), while the limited scale and capabilities of the base models further restrict the model performance. The third approach (Fu et al., 2024; Wu et al., 2024) involves extending pre-trained MoE-based LLMs with multimodal capabilities, thus avoiding the computational burden of training from scratch and mitigating constraints from the original model’s linguistic capacity. Furthermore, (Lo et al., 2024) indicates that such MoE models, having been pretrained on large-scale text corpora, already exhibit well-differentiated expert knowledge, thereby reducing the likelihood of redundant expert specialization during multimodal adaptation. Therefore, we hold the view that the third approach offers higher feasibility for obtaining MLLMs with MoE architectures.

However, a notable challenge during multimodal transfer training is the potential degradation of the model’s language capabilities. Previous works such as VITA (Fu et al., 2024) and DeepSeek-VL2 (Liu et al., 2024) incorporate approximately 20% pure textual data during multimodal training to help preserve the model’s language capabilities. Nevertheless, this strategy not only increases the training time cost, but also raises the acquisition cost of high-quality textual data during multimodal training. Other works (Long et al., 2024) have explored

modality expansion by incorporating efficient finetuning modules while freezing the backbone of the language model to preserve its original language capabilities. However, due to the limited number of tunable parameters in these modules, the multimodal performance ceiling of the model is often constrained.

Consequently, reducing the reliance on textual data while preserving language capabilities remains a significant challenge in building effective MLLMs. In this paper, we propose a novel modality-aware routing strategy to address this issue. Previous studies (Li et al., 2025) have shown that in MoE-based MLLMs, experts tend to exhibit modality preferences, resulting in notable differences in the probability of routing tokens from different modalities to the same expert. This observation motivates us to explore modality-aware routing strategies that explicitly control modality preferences in the routing mechanism, thereby encouraging the specialization of experts in modality-specific knowledge and ultimately helping to preserve linguistic capabilities. However, most existing MoE-based MLLMs predominantly employ routing under load-balancing loss constraints or resort to manually enforced hard partitioning of modality-specific experts (Luo et al., 2024). This rigid partitioning will split the original knowledge areas of experts, making it difficult to determine the optimal grouping strategy, thus failing to achieve the goal of maintaining strong language performance.

Motivated by the above considerations, we design a statistical method to characterize the routing probability distributions across tokens from different modalities (modality routing distribution, MRD). Based on these distributions, we compute the distance between the routing probability distributions of different modality tokens using the Kullback–Leibler divergence and introduce an auxiliary loss to constrain this divergence. Without any modifications to the data or model architecture, we manually control the modality preferences of the model’s experts, which effectively helps to preserve the model’s language capabilities. Moreover, unlike conventional finetuning approaches, our method does not require freezing the model backbone to preserve language capabilities, thereby fully unleashing the model’s multimodal performance potential.

Our contributions can be summarized as follows:

- We propose a novel metric for evaluating

the routing probability distributions of tokens from different modalities, introducing a new perspective for analyzing routing strategies in MoE-based multimodal models.

- Based on the understanding of modality routing probability distributions, we employ the Kullback–Leibler divergence to measure the MRD distance and impose a constraint through the Soft Modality-Aware Routing (SMAR) loss. This method allows explicit control over the degree of expert modality differentiation without requiring any architectural modifications.
- Extensive experiments demonstrate that controlling expert modality differentiation during multimodal training via SMAR reduces the impact of data distribution on expert specialization. SMAR achieves strong multimodal performance and attains a language capability retention rate of 86.6% on visual instruction finetuning data with only 2.5% pure text, outperforming both the baseline without auxiliary loss (81.6%) and the model using load balancing loss alone (82.8%).

2 Related Works

2.1 Preserving Language Capabilities in MLLMs

Research on maintaining language capabilities in MLLMs is still in its early stages. Most mainstream approaches for preserving language capabilities rely on increasing the proportion of pure-text instruction fine-tuning data, as exemplified by models such as Qwen2-VL (Wang et al., 2024) and DeepSeek-VL2 (Wu et al., 2024). Although freezing the LLM backbone and employing efficient fine-tuning modules such as LoRA (Hu et al., 2022) can endow the model with multimodal capabilities while preserving much of its language proficiency, the limited number of tunable parameters in these methods tends to restrict the model’s multimodal performance ceiling, particularly during large-scale training.

In contrast, we seek to explore a more cost-effective approach with a higher multimodal performance ceiling. SMAR leverages the inherent advantages of the MoE architecture by controlling the differentiation of modality preference among experts to store knowledge specific to different modalities. This enables the preservation of language capabilities while maintaining strong multimodal

performance.

2.2 MoE Routing Strategy in MLLMs

Current research on modality-aware routing strategies is limited. For instance, Mono-InternVL (Luo et al., 2024) uses a rule-based hard routing that maps image and text tokens exclusively to corresponding experts, necessitating extensive visual pretraining data. Similarly, VL-MoE (Shen et al., 2023) separates visual and textual experts in lower layers and fuses them at higher layers, combining modality-specific feature separation with semantic fusion. However, both methods require significant architectural modifications, limiting their applicability to existing MoE-based large language models. Flex-MoE (Yun et al., 2024) proposes a relatively soft modality-distinguished routing strategy by predefining the number of experts corresponding to each modality according to the modality count. It computes a cross-entropy loss based on the tokens’ modality labels and their routing probabilities to encourage modality-specific routing. However, this approach still requires manual specification of the number of experts per modality and lacks a global understanding of the overall distribution of routing probabilities as a constraint.

3 Method

We propose a soft modality-aware routing strategy for MoE-MLLMs. First, we define the **Modality Routing Distribution (MRD)** to capture routing patterns per modality. Second, we introduce the **Soft Modality-Aware Routing (SMAR)** loss, which uses the KL divergence to regularize the MRD and thereby control experts’ modality preferences. Then, we provide an explanation of how this loss is integrated with standard objectives. Finally, we describe the model architecture and the two-stage training strategy.

Our goal is to have some experts specialize in pure language tasks, others focus on vision tasks, and yet others act as multimodal fusion experts handling large amounts of both textual and visual information. We do not explicitly assign which experts should take on each role. Instead, the model autonomously selects and differentiates expert responsibilities under the **soft constraints** imposed by SMAR.

3.1 Modality-Aware Routing Distribution

Consider a mini-batch containing N tokens, among which N_v are visual and N_t are textual ($N = N_v +$

N_t). Let $\mathbf{C} \in \mathbb{R}^{N \times H}$ be the hidden states, where H is the hidden dimension. In a MoE Decoder layer such as the one used in Mixtral 8x7B (Jiang et al., 2024), each token is routed to a subset of E feed-forward experts. We denote the router network by $g(\cdot)$ and index experts with $e \in \{1, \dots, E\}$.

Router logits. To explicitly control modality preference, we introduce trainable **modality-aware bias** vectors $\mathbf{b}_v, \mathbf{b}_t \in \mathbb{R}^E$ for vision and text, respectively. The router logits for the two modalities are

$$\mathbf{L}_v = g(\mathbf{C}_v) + \mathbf{1} \mathbf{b}_v^\top \in \mathbb{R}^{N_v \times E}, \quad (1)$$

$$\mathbf{L}_t = g(\mathbf{C}_t) + \mathbf{1} \mathbf{b}_t^\top \in \mathbb{R}^{N_t \times E}, \quad (2)$$

$$\mathbf{L} = \text{concat}(\mathbf{L}_v, \mathbf{L}_t) \in \mathbb{R}^{N \times E}. \quad (3)$$

where $\mathbf{1}$ is an all-ones column vector whose length matches the number of tokens in the corresponding modality.

Routing probabilities. For each token i , the softmax over experts yields

$$P_{i,e} = \text{softmax}(\mathbf{L}_{i,:})_e = \frac{\exp(\mathbf{L}_{i,e})}{\sum_{e'=1}^E \exp(\mathbf{L}_{i,e'})}. \quad (4)$$

Top- K selection. Following sparse MoE practice, we pick the K experts with the largest $P_{i,e}$: $T_i = \{r_1, \dots, r_K\} \subseteq \{1, \dots, E\}$. The weights are renormalised within T_i ,

$$\hat{w}_{i,e} = \begin{cases} \frac{P_{i,e}}{\sum_{e' \in T_i} P_{i,e'}}, & e \in T_i, \\ 0, & e \notin T_i. \end{cases} \quad (5)$$

Frequency and expected weight. Let $\mathcal{I}_m = \{i \mid \text{token } i \text{ is modality } m\}$ and $N_m = |\mathcal{I}_m|$. For each modality $m \in \{v, t\}$ we compute

$$F_{m,e} = \frac{1}{KN_m} \sum_{i \in \mathcal{I}_m} \mathbf{1}[e \in T_i], \quad (6)$$

$$R_{m,e} = \frac{1}{N_m} \sum_{i \in \mathcal{I}_m} \hat{w}_{i,e}. \quad (7)$$

Modality Routing Distribution. The unnormalised expert mass is $Q_{m,e} = F_{m,e} R_{m,e}$. Normalising over E experts yields the *Modality Routing Distribution (MRD)*.

$$\tilde{Q}_{m,e} = \frac{Q_{m,e}}{\sum_{e'=1}^E Q_{m,e'}}, \quad (8)$$

$$\tilde{\mathbf{q}}_m = (\tilde{Q}_{m,1}, \dots, \tilde{Q}_{m,E}). \quad (9)$$

We write $\tilde{\mathbf{q}}_v$ and $\tilde{\mathbf{q}}_t$ for vision and text, respectively.

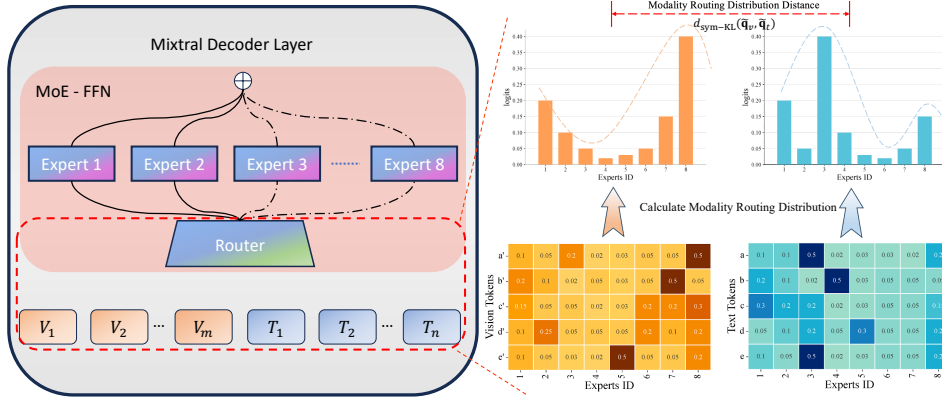


Figure 1: **Illustration of the proposed Soft Modality-Aware Routing (SMAR) mechanism inside a single Mixtral decoder layer.** **Left:** Visual tokens $\{V_1, \dots, V_m\}$ (orange) and textual tokens $\{T_1, \dots, T_n\}$ (blue) are fed into the shared MoE-FFN. The router selects the Top- K experts for each token (dashed arrows). **Right:** The token-expert matrix (heat-map) represents the router logits of each token. We calculate the modality routing distribution by our method and the symmetric KL divergence $d_{\text{sym-KL}}(\tilde{\mathbf{q}}_v, \tilde{\mathbf{q}}_t)$ (red bracket) quantifies the cross-modal routing gap and is kept within a tolerance band—by the SMAR loss (Eq. 13).

3.2 Soft Modality-Aware Routing Loss

The symmetric Kullback–Leibler divergence between the two routing distributions is

$$d_{\text{sym-KL}} = \frac{1}{2} \left(\text{KL}(\tilde{\mathbf{q}}_v \| \tilde{\mathbf{q}}_t) + \text{KL}(\tilde{\mathbf{q}}_t \| \tilde{\mathbf{q}}_v) \right), \quad (10)$$

$$\text{KL}(\tilde{\mathbf{q}}_v \| \tilde{\mathbf{q}}_t) = \sum_{e=1}^E \tilde{Q}_{v,e} \log \frac{\tilde{Q}_{v,e}}{\tilde{Q}_{t,e}}, \quad (11)$$

$$\text{KL}(\tilde{\mathbf{q}}_t \| \tilde{\mathbf{q}}_v) = \sum_{e=1}^E \tilde{Q}_{t,e} \log \frac{\tilde{Q}_{t,e}}{\tilde{Q}_{v,e}}. \quad (12)$$

We impose a tolerance band $[d_{\min}, d_{\max}]$ on $d_{\text{sym-KL}}$ and penalise violations via the *Soft Modality-Aware Routing (SMAR)* loss:

$$\mathcal{L}_{\text{SMAR}} = \begin{cases} d_{\min} - d_{\text{sym-KL}}, & d_{\text{sym-KL}} < d_{\min}, \\ d_{\text{sym-KL}} - d_{\max}, & d_{\text{sym-KL}} > d_{\max}, \\ 0, & \text{otherwise.} \end{cases} \quad (13)$$

3.3 Overall Training Objective

The final loss combines the primary task loss $\mathcal{L}_{\text{main}}$, the standard load-balancing loss $\mathcal{L}_{\text{balance}}$ (Fedus et al., 2022), and the proposed SMAR loss:

$$\mathcal{L}_{\text{total}} = \mathcal{L}_{\text{main}} + \alpha \mathcal{L}_{\text{balance}} + \beta \mathcal{L}_{\text{SMAR}}, \quad (14)$$

where α and β are hyper-parameters controlling the relative strength of the auxiliary terms.

3.4 Model Architecture

We inherit the overall design of VITA (Fu et al., 2024) but restrict the modalities to vision and text owing to computational constraints. The language backbone is Mixtral 8x7B (Jiang et al., 2024) while the vision branch is instantiated with InternViT-300M (Chen et al., 2024) at an input resolution of 448 px. For high-resolution images, we adopt VITA’s dynamic tiling strategy, partitioning each image into non-overlapping 448 px tiles. Every tile is encoded into a sequence of visual tokens, which are subsequently linearly projected by a two-layer MLP connector and concatenated with the textual tokens before being fed into the language model.

3.5 Training Strategy

Following the two-stage curriculum popularized by LLaVA-1.5 (Liu et al., 2023b), we first perform *visual alignment*, where the language backbone and visual encoder are frozen and only the MLP connector is trained to align visual and textual token representations. Next, during *visual instruction tuning*, the visual encoder remains fixed while both the language backbone and connector are fine-tuned on multimodal instruction data to improve instruction-following ability. The composition of the training corpus and additional implementation details are provided in Section 4.

4 Experiments

4.1 Experimental Setup

Datasets. Following MoE-LLaVA (Lin et al., 2024), we use the pretrained data of LLaVA 1.5-

Table 1: Comparison among different LVLMs on multimodal benchmarks and language benchmarks. "Res.", "Act.", "V", "P", "M" respectively represent the input image resolution, activated parameters, Vicuna (Chiang et al., 2023), Phi-2 (Jawaheripi et al., 2023), Mixtral (Jiang et al., 2024). The best results and second best results are indicated by boldface and underline, respectively.

Method	LLM	Act.	Res.	Multimodal Capabilities								Language Capabilities															
				VQA ^{v2}	GQA	VizWiz	SQA ^I	VQA ^T	POPE	MME	MMB	MM-Vet	MMLU	C-EVAL	GSM8K	BBH	ARC_c	MBPP	HumanEval	IFEval							
<i>Base Model</i>																											
Vicuna-7B (Chiang et al., 2023)	V-7B	7B	-	-	-	-	-	-	-	-	-	-	-	-	-	-	-	-	-	47.4	36.7	23.4	41.4	39.3	13.8	19.5	40.8
Vicuna-13B (Chiang et al., 2023)	V-13B	13B	-	-	-	-	-	-	-	-	-	-	-	-	-	-	-	-	-	53.9	35.0	38.1	50.1	52.5	3.6	16.5	50.3
Phi-2 (Jawaheripi et al., 2023)	P-2.7B	2.7B	-	-	-	-	-	-	-	-	-	-	-	-	-	-	-	-	-	58.5	30.6	61.6	59.3	53.2	49.2	30.5	27.7
Mixtral 8x7B (Jiang et al., 2024)	M 8x7B	13B	-	-	-	-	-	-	-	-	-	-	-	-	-	-	-	-	-	72.0	55.0	67.2	68.8	82.0	49.0	23.2	22.2
<i>Dense Model</i>																											
LLaVA-1.5 (Liu et al., 2023b)	V-7B	7B	336	78.5	62.0	50.0	66.8	58.2	85.9	1510.7	64.3	30.5	46.3	22.7	19.5	41.5	30.9	-	-	51.7	19.1	34.2	48.0	38.3	-	17.7	39.4
LLaVA-1.5 (Liu et al., 2023b)	V-13B	13B	336	80.0	63.3	53.6	71.6	61.3	85.9	1531.3	67.7	35.4	51.7	19.1	34.2	48.0	38.3	-	-	51.7	19.1	34.2	48.0	38.3	-	21.3	48.9
<i>Sparse Model</i>																											
MoE-LLaVA-2.7Bx4-Top2 (Lin et al., 2024)	P-2.7B	3.6B	384	79.9	62.6	43.7	70.3	57.0	85.7	1431.3	68.0	35.9	49.0	30.2	51.7	52.5	70.9	43.4	51.2	49.0	30.2	51.7	52.5	70.9	43.4	51.2	35.4
Baseline	M 8x7B	13B	448	82.5	62.2	53.7	74.6	69.6	86.8	1634.7	72.0	32.9	67.6	47.4	57.1	62.0	77.0	10.4	46.3	67.6	47.4	57.1	62.0	77.0	10.4	46.3	48.7
Baseline w/ $\mathcal{L}_{\text{balance}}$	M 8x7B	13B	448	82.5	62.5	<u>55.0</u>	74.5	69.8	86.4	1600.6	<u>72.4</u>	39.4	67.8	45.9	56.6	60.2	81.0	14.8	43.9	67.8	45.9	56.6	60.2	81.0	14.8	43.9	47.5
Baseline w/ SMAR	M 8x7B	13B	448	<u>82.4</u>	<u>62.4</u>	55.1	75.5	69.2	<u>86.6</u>	1638.8	72.7	<u>35.9</u>	68.0	<u>46.8</u>	<u>57.0</u>	<u>61.8</u>	<u>79.3</u>	28.4	49.4	68.0	<u>46.8</u>	<u>57.0</u>	<u>61.8</u>	<u>79.3</u>	28.4	49.4	50.7

558k (Liu et al., 2023b) for the visual alignment stage. And we use the datasets from MIMIC-IT (Li et al., 2023a), LRV (Liu et al., 2023a), SViT (Zhao et al., 2023), LVIS (Wang et al., 2023) and LLaVA-mix-665k (Liu et al., 2023b) for the instruction tuning stage. The proportion of text-only data in visual instruction tuning stage is only 2.5%. More information is detailed in the appendix A.

Training implementation. We adopt a two-stage training protocol. In Stage 1, the model is trained with a batch size of 128, a learning rate of $5e-4$. Stage 2 uses a larger batch size of 256 and a reduced learning rate of $2e-5$ with the same scheduling strategy. The SMAR loss parameters $[d_{\min}, d_{\max}]$ are applied starting from Stage 2, set to $[1.5, 2.0]$, with $\beta = 0.01$. Additional training configurations and hyperparameters are detailed in the appendix A.

4.2 Evaluation Details

We evaluate the multimodal capabilities of our model across a diverse set of multimodal tasks. For general multimodal question answering (QA), we benchmark performance on VQA-v2 (Goyal et al., 2017), MME (Fu et al., 2023), and ScienceQA-IMG (Lu et al., 2022). To evaluate the optical character recognition (OCR) capabilities, we use TextVQA (Singh et al., 2019) and VizWiz (Gurari et al., 2018). For reasoning and fine-grained visual understanding, we evaluate on GQA (Hudson and Manning, 2019), MM-Vet (Yu et al., 2023), and MMBench (Liu et al., 2023c). Additionally, we employ the POPE (Li et al., 2023b) benchmark to measure the model’s propensity for hallucination.

We also use a diverse set of benchmarks to evaluate the language capabilities of the proposed model. These include evaluations of general knowledge (MMLU (Hendrycks et al., 2020), C-EVAL (Huang

et al., 2023)), mathematical (GSM8K (Cobbe et al., 2021)) and reasoning abilities (BBH (Suzgun et al., 2022), ARC-Challenge (Clark et al., 2018)). Moreover, we evaluate the coding proficiency (MBPP (Austin et al., 2021), HumanEval (Chen et al., 2021)) and instruction-following capabilities (IFEval (Zhou et al., 2023)). All language capability evaluations are performed using the OpenCompass toolkit.

4.3 Results

Multimodal Performance. As shown in Table 1, our model demonstrates strong multimodal capabilities, largely outperforming LLaVA-1.5-13B (Liu et al., 2023b), a model with a comparable number of activated parameters, across a comprehensive suite of benchmarks. Specifically, on SQA^I, MME, MMBench, MM-Vet, VQA^T, and VQA^{v2}, our model achieves performance gains of 5.4%, 7.0%, 7.4%, 12.8%, and 3.0%, respectively, over LLaVA-1.5-13B. This robust performance underscores its proficiency in handling common multimodal tasks, including general visual question answering, optical character recognition, and understanding scene relationships. Furthermore, when compared against other approaches employing identical datasets and model architectures, SMAR also gets the best results on several metrics across VizWiz, SQA^I, MME, and MMBench.

Preservation of Language Capabilities. As shown in Table 1, our SMAR method achieves leading performance on benchmarks such as MMLU, MBPP, HumanEval, and IFEval, and attains competitive (second-best) performance on other evaluated tasks.

To isolate the models’ language capabilities from gains stemming from instruction tuning, we average performance exclusively across six

Table 2: Language capability retention ratio comparison among different methods.

Method	LLM	MMLU	CEVAL	GSM8K	BBH	ARC_c	MBPP	Avg.
Vicuna-13B	V-13B	53.9	35.0	38.1	50.1	52.5	3.6	38.9
LLaVA-1.5	V-13B	51.7	19.1	34.2	48.0	38.3	0.0	31.9
Retention ratio %		95.9	54.6	89.8	95.8	73.0	0.0	82.0
Mixtral 8x7B	M 8x7B	72.0	55.0	67.2	68.8	82.0	49.0	65.7
Baseline	M 8x7B	67.6	47.4	57.1	62.0	77.0	10.4	53.6
Retention ratio %		93.9	86.2	85.0	90.1	93.9	21.2	81.6
Baseline w/ $\mathcal{L}_{\text{balance}}$	M 8x7B	67.8	45.9	56.6	60.2	81.0	14.8	54.4
Retention ratio %		94.2	83.5	84.2	87.5	98.8	30.2	82.8
Baseline w/ SMAR	M 8x7B	68.0	46.8	57.0	61.8	79.3	28.4	56.9
Retention ratio %		94.4	85.1	84.8	89.8	96.7	58.0	86.6

benchmarks (C-EVAL, MMLU, GSM8K, ARC-Challenge, BBH, and MBPP) that have minimal impact on instruction-following capability to compute the retention ratio of language capabilities, as shown in Table 2. With 6.0% of its instruction-tuning corpus consisting of pure-text prompts, LLaVA-1.5-13B retains 82.0% of the backbone’s original language capabilities.

Using only 2.5% pure-text data, SMAR still preserves 86.6%—clearly surpassing both the no-auxiliary-loss variant (81.6%) and the load-balancing-only variant (82.8%).

Notably, in code-related evaluations, SMAR demonstrates substantial improvements: its MBPP performance is nearly double that of the model trained with only load-balancing loss. Concurrently, SMAR also outperforms configurations with only load-balancing loss and with no auxiliary losses by 12.5% and 6.7% on HumanEval as shown in Table 1, respectively. In particular, our multimodal models’ backbone is initialized from a base model *without* prior instruction tuning and the preservation of code formatting is likely correlated with instruction-following capabilities. We hypothesize that SMAR enhances instruction-following capability. This is supported by a 6.7% improvement on the IFEval benchmark for SMAR compared to using only load-balancing loss. These improvements may stem from the relatively stringent lower bound we impose on the modal routing distribution distance within SMAR, which encourages modality-specific expert specialization and enhances their sensitivity to linguistic cues in instructions.

As shown in Table 1, LLaVA-1.5 struggles to adhere to specified code formats from examples, resulting in a failure to score on the MBPP benchmark. On knowledge-intensive benchmarks like C-EVAL, its performance drops substantially; LLaVA-1.5-13B, for example, retains only 54.5% of its base model’s performance, a decline po-

tentially attributable to the limited proportion of Chinese data. For complex reasoning tasks, such as ARC-Challenge (ARC_c), it preserves merely 73.0% of its original performance. Dense models such as LLaVA-1.5, where text-only instruction fine-tuning data constitutes a small fraction (e.g., 6.0%) of the training corpus, often exhibit significant degradation in language capabilities.

In contrast, our approach utilizes the MoE architecture. When employing only the standard load-balancing loss, performance on ARC-Challenge remains nearly on par with the original base model. When trained without specific auxiliary losses aimed at language preservation, this MoE architecture inherently demonstrates greater resilience to language capabilities degradation from multimodal inputs. However, coding ability is notably harmed under this basic setup, with MBPP performance dropping to 30.2%. The introduction of our SMAR method yields a near two-fold improvement on MBPP, effectively alleviating the issue of code format adherence.

Generalisability of SMAR. To validate the generalizability of SMAR across different architectures, we integrate it into MoE-LLaVA. Results are reported in Table 3. To minimize interference from extraneous factors, we build upon the publicly released weights from MoE-LLaVA’s first-stage connector and their second-stage visually instruction-finetuned model. Our training is conducted exclusively in the third stage as defined in their work, focusing solely on the MoE expansion process by training only the model’s FFN experts and gating network.

We trained two versions of the model: one strictly following the original MoE-LLaVA training protocol, and the other incorporating the SMAR loss during the third training stage. When applying SMAR to MoE-LLaVA, we set d_{min} to 1.0 and d_{max} to 1.5 encourage modality-based expert differentiation, with the weighting factor β set to 0.01 and all other components remained unchanged.

MoE-LLaVA, in its multimodal training, employs an upgrade strategy where FFN layers from the original dense base model are fully replicated for its experts. Theoretically, each such expert FFN retains the full knowledge of the precursor language model, leading to comparatively minor degradation in language capabilities.

Experimental results demonstrate that SMAR effectively preserves language capabilities, achieving

Table 3: **Comparison among different methods applied on MoE-LLaVA.** † represent that we reproduced the training of MoE-LLaVA following original settings. "w/ SMAR" means that we apply SMAR loss to MoE-LLaVA.

Method	Multimodal Capabilities									Language Capabilities						
	VQA ^{v2}	GQA	VizWiz	SQA ¹	VQA ¹	POPE	MME	MMB	MM-Vet	MMLU	C-EVAL	GSM8K	BBH	ARC_c	MBPP	HumanEval
Phi-2 (Jawaheripi et al., 2023)	-	-	-	-	-	-	-	-	-	58.5	30.6	61.6	59.3	53.2	49.2	30.5
MoE-LLaVA-2.7Bx4-Top2 (Lin et al., 2024)	79.9	62.6	43.7	70.3	57.0	85.7	1431.3	68.0	35.9	49.0	30.2	51.7	<u>52.5</u>	70.9	43.4	51.2
MoE-LLaVA-2.7Bx4-Top2 [†]	<u>78.9</u>	<u>61.9</u>	38.0	70.3	55.2	85.7	1402.1	68.3	34.2	<u>52.5</u>	<u>30.3</u>	<u>53.5</u>	52.4	<u>72.9</u>	40.6	52.4
w/ SMAR	<u>78.9</u>	60.7	<u>40.3</u>	70.3	<u>56.3</u>	84.5	1420.0	67.6	<u>35.4</u>	53.7	31.9	55.4	53.1	73.2	41.0	<u>51.8</u>

the best performance across multiple benchmarks including MMLU, C-EVAL, GSM8K, BBH, and ARC-Challenge. Although its multimodal performance metrics do not fully match those reported for MoE-LLaVA, comparison with our reproduced MoE-LLaVA experiments indicates that SMAR contributes to improvements in certain aspects of multimodal performance.

4.4 Ablation Study

Table 4: **Ablation of different lower bound(d_{min}) and upper bound(d_{max}) settings.**

d_{min}, d_{max}	Multimodal Capabilities					Language Capabilities				
	MME	SQA	TextQA	GQA	MMB	MMLU	GSM8K	BBH	MBPP	HumanEval
0.1, 0.5	1606.1	73.7	70.0	62.1	71.2	65.6	56.8	62.3	15.8	45.7
0.5, 1.0	1622.6	73.3	69.3	<u>62.4</u>	72.5	66.3	58.2	<u>62.2</u>	9.2	47.6
1.0, 1.5	<u>1636.7</u>	<u>74.4</u>	<u>69.7</u>	62.5	72.9	<u>67.0</u>	54.1	61.5	36.4	46.3
1.5, 2.0	1638.8	75.5	69.2	<u>62.4</u>	<u>72.7</u>	68.0	<u>57.0</u>	61.8	<u>28.4</u>	49.4

Ablation on SMAR Thresholds. We investigate the influence of the d_{min} and d_{max} by evaluating several pairs of values. The results are summarised in Table 4. The best overall language score is obtained for $d_{min} = 1.5$ and $d_{max} = 2.0$.

To gain intuition, we visualise the layer-wise MRD distance for each threshold setting in Figure 2. The MRD distance is computed from the 2,300 evaluation samples in the MME benchmark. The most notable change occurs in the maximum MRD distance, which increases significantly as the threshold range expands. However, when the lower bound of the SMAR threshold is set too high, the distribution curve of the MRD distance shows little variation, and the difference in mean values diminishes. This may be due to the excessively stringent requirement for expert modality differentiation, which is difficult to achieve through training alone.

We further compare the MRD of the best SMAR model with two baseline variants that do not employ SMAR as shown in Figure 3. Clear changes in routing strategy emerge. In Figure 4 we plot the proportion of image and text tokens routed to each expert at every layer. After activating SMAR, several experts develop pronounced modality preferences. For instance, Expert 8 in Layer 13 almost exclusively processes text tokens, as shown in Fig-

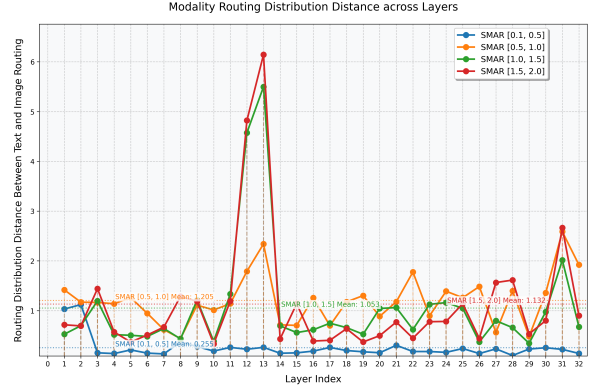


Figure 2: **The MRD distance curve of different $[d_{min}, d_{max}]$ settings.** We observe that the MRD curves exhibit significant changes in response to different threshold settings.

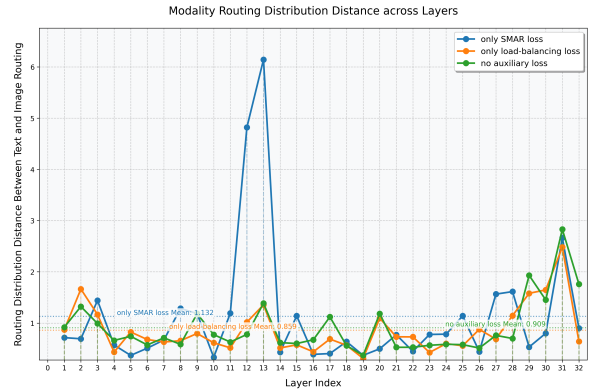


Figure 3: **The MRD distance curve of different methods.** It is evident that after applying the SMAR method to encourage modality-specific expert differentiation, the MRD curves differ significantly from those observed in methods without SMAR.

Table 5: **Ablation of modality-specific bias and load-balancing loss on SMAR.**

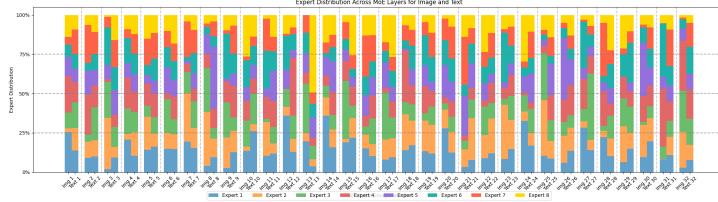
d_{min}, d_{max}	Modality-Aware Bias	Load-Balancing Loss	MMLU	GSM8K	BBH	ARC_c	MBPP
1.0, 1.5	No	No	63.9	54.5	62.0	79.7	17.4
1.0, 1.5	Yes	No	67.0	54.1	<u>61.5</u>	<u>80.3</u>	36.4
1.0, 1.5	Yes	Yes	<u>65.0</u>	56.0	61.7	81.0	18.8

ure 4b.

We also find that the routing collapse occurs on the model that is applied with the lowest thresholds ($d_{min} = 0.1, d_{max} = 0.5$). As shown in Figure 4c, the tokens tend to be routed to the same expert, leading to the worst performance.



(a) The experts exhibit naturally emerging modality preferences with load-balancing loss.



(b) With the $[d_{min}, d_{max}]$ set to $[1.5, 2.0]$, many experts across multiple layers exhibit more pronounced modality preferences—for instance, Expert 8 in layer 13 serves almost exclusively text tokens.



(c) When the threshold is set to $[0.1, 0.5]$, severe routing collapse occurs in all layers starting from layer 3.

Figure 4: **The detailed depiction of the proportion of image and text tokens routed to each expert at every layer.** (a) illustrates the modality preferences of experts across layers in the model trained solely with the load-balancing loss. (b) demonstrates the effectiveness of the SMAR method in controlling expert modality preferences. (c) shows that setting the threshold too low can lead to routing collapse in the model.

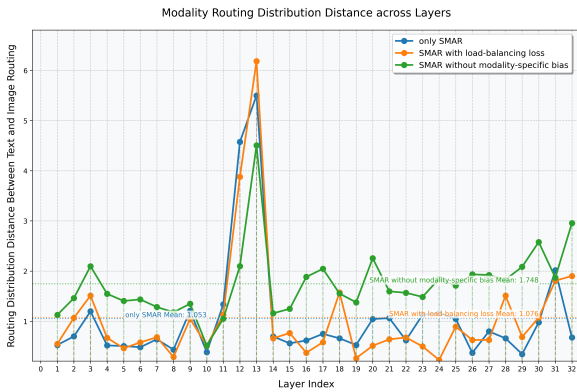


Figure 5: **The MRD distance curve illustrating the effects of applying Modality-Specific Bias and the load-balancing loss within the SMAR framework.**

Effect of the Trainable Modality-Aware Bias and the Load-Balancing Loss. Table 5 presents an ablation in which the trainable modality-aware bias and the conventional load-balancing loss are toggled on and off while keeping the SMAR thresholds fixed. Adding modality-aware bias consistently improves performance. Conversely, introducing the load-balancing loss degrades the results,

which explains why we omit it in the final model.

The corresponding MRD distance plots are provided in Figure 5. A modality-aware bias slightly lowers token-modality separation, whereas the load-balancing loss results in a decrease in the minimum MRD distance of the model.

5 Conclusion

In this work, we propose a novel perspective, **MRD** for analyzing the routing behavior of different modality tokens in MoE-MLLMs. Building upon this, we introduce the **SMAR** to regulate the degree of modality differentiation among experts. By encouraging modality-specific expert specialization, our method acquires strong multimodal performance and achieves improved preservation of language capabilities without additional pure text data or freezing the backbone.

6 Limitations

Despite our contributions, this work has certain limitations. Firstly, the proposed MRD and SMAR loss are not restricted by the number of modalities.

However, our current implementation and evaluation are confined to vision-language modality. The efficacy of SMAR in balancing capabilities across a broader spectrum of modalities remains an avenue for future exploration. Secondly, our method introduces two hyperparameters that require tuning: the thresholds for the MRD distance (lower and upper bounds) and the trade-off coefficient for the SMAR loss. Due to computational resource constraints, we have conducted limited exploration of hyperparameter sensitivity across different MoE-MLLMs. We leave exploration of these two limitations to future work.

References

- Jacob Austin, Augustus Odena, Maxwell Nye, Maarten Bosma, Henryk Michalewski, David Dohan, Ellen Jiang, Carrie Cai, Michael Terry, Quoc Le, and 1 others. 2021. Program synthesis with large language models. *arXiv preprint arXiv:2108.07732*.
- Mark Chen, Jerry Tworek, Heewoo Jun, Qiming Yuan, Henrique Ponde De Oliveira Pinto, Jared Kaplan, Harri Edwards, Yuri Burda, Nicholas Joseph, Greg Brockman, and 1 others. 2021. Evaluating large language models trained on code. *arXiv preprint arXiv:2107.03374*.
- Zhe Chen, Jiannan Wu, Wenhai Wang, Weijie Su, Guo Chen, Sen Xing, Muyan Zhong, Qinglong Zhang, Xizhou Zhu, Lewei Lu, and 1 others. 2024. Internvl: Scaling up vision foundation models and aligning for generic visual-linguistic tasks. In *Proceedings of the IEEE/CVF conference on computer vision and pattern recognition*, pages 24185–24198.
- Wei-Lin Chiang, Zhuohan Li, Ziqing Lin, Ying Sheng, Zhanghao Wu, Hao Zhang, Lianmin Zheng, Siyuan Zhuang, Yonghao Zhuang, Joseph E Gonzalez, and 1 others. 2023. Vicuna: An open-source chatbot impressing gpt-4 with 90%* chatgpt quality. See <https://vicuna.lmsys.org> (accessed 14 April 2023), 2(3):6.
- Peter Clark, Isaac Cowhey, Oren Etzioni, Tushar Khot, Ashish Sabharwal, Carissa Schoenick, and Oyvind Tafjord. 2018. Think you have solved question answering? try arc, the ai2 reasoning challenge. *arXiv preprint arXiv:1803.05457*.
- Karl Cobbe, Vineet Kosaraju, Mohammad Bavarian, Mark Chen, Heewoo Jun, Lukasz Kaiser, Matthias Plappert, Jerry Tworek, Jacob Hilton, Reiichiro Nakano, and 1 others. 2021. Training verifiers to solve math word problems. *arXiv preprint arXiv:2110.14168*.
- William Fedus, Barret Zoph, and Noam Shazeer. 2022. Switch transformers: Scaling to trillion parameter models with simple and efficient sparsity. *Journal of Machine Learning Research*, 23(120):1–39.
- Chaoyou Fu, Peixian Chen, Yunhang Shen, Yulei Qin, Mengdan Zhang, Xu Lin, Jinrui Yang, Xiaowu Zheng, Ke Li, Xing Sun, and 1 others. 2023. Mme: A comprehensive evaluation benchmark for multimodal large language models. *arXiv preprint arXiv:2306.13394*.
- Chaoyou Fu, Haojia Lin, Zuwei Long, Yunhang Shen, Meng Zhao, Yifan Zhang, Shaoqi Dong, Xiong Wang, Di Yin, Long Ma, and 1 others. 2024. Vita: Towards open-source interactive omni multimodal llm. *arXiv preprint arXiv:2408.05211*.
- Yash Goyal, Tejas Khot, Douglas Summers-Stay, Dhruv Batra, and Devi Parikh. 2017. Making the v in vqa matter: Elevating the role of image understanding in visual question answering. In *Proceedings of the IEEE conference on computer vision and pattern recognition*, pages 6904–6913.
- Danna Gurari, Qing Li, Abigale J Stangl, Anhong Guo, Chi Lin, Kristen Grauman, Jiebo Luo, and Jeffrey P Bigham. 2018. Vizwiz grand challenge: Answering visual questions from blind people. In *Proceedings of the IEEE conference on computer vision and pattern recognition*, pages 3608–3617.
- Dan Hendrycks, Collin Burns, Steven Basart, Andy Zou, Mantas Mazeika, Dawn Song, and Jacob Steinhardt. 2020. Measuring massive multitask language understanding. *arXiv preprint arXiv:2009.03300*.
- Edward J Hu, Yelong Shen, Phillip Wallis, Zeyuan Allen-Zhu, Yuanzhi Li, Shean Wang, Lu Wang, Weizhu Chen, and 1 others. 2022. Lora: Low-rank adaptation of large language models. *ICLR*, 1(2):3.
- Yongqi Huang, Peng Ye, Chenyu Huang, Jianjian Cao, Lin Zhang, Baopu Li, Gang Yu, and Tao Chen. 2025. Ders: Towards extremely efficient upcycled mixture-of-experts models. *arXiv preprint arXiv:2503.01359*.
- Yuzhen Huang, Yuzhuo Bai, Zhihao Zhu, Junlei Zhang, Jinghan Zhang, Tangjun Su, Junteng Liu, Chuancheng Lv, Yikai Zhang, Yao Fu, and 1 others. 2023. C-eval: A multi-level multi-discipline chinese evaluation suite for foundation models. *Advances in Neural Information Processing Systems*, 36:62991–63010.
- Drew A Hudson and Christopher D Manning. 2019. Gqa: A new dataset for real-world visual reasoning and compositional question answering. In *Proceedings of the IEEE/CVF conference on computer vision and pattern recognition*, pages 6700–6709.
- Mojan Javaheripi, Sébastien Bubeck, Marah Abdin, Jyoti Aneja, Sébastien Bubeck, Caio César Teodoro Mendes, Weizhu Chen, Allie Del Giorno, Ronen Eldan, Sivakanth Gopi, and 1 others. 2023. Phi-2: The surprising power of small language models. *Microsoft Research Blog*, 1(3):3.
- Albert Q Jiang, Alexandre Sablayrolles, Antoine Roux, Arthur Mensch, Blanche Savary, Chris Bamford, Devendra Singh Chaplot, Diego de las Casas,

- Emma Bou Hanna, Florian Bressand, and 1 others. 2024. Mixtral of experts. *arXiv preprint arXiv:2401.04088*.
- Bo Li, Yuanhan Zhang, Liangyu Chen, Jinghao Wang, Fanyi Pu, Jingkang Yang, Chunyuan Li, and Ziwei Liu. 2023a. Mimic-it: Multi-modal in-context instruction tuning. *arXiv preprint arXiv:2306.05425*.
- Dongxu Li, Yudong Liu, Haoning Wu, Yue Wang, Zhiqi Shen, Bowen Qu, Xinyao Niu, Fan Zhou, Chengen Huang, Yanpeng Li, and 1 others. 2024. Aria: An open multimodal native mixture-of-experts model. *arXiv preprint arXiv:2410.05993*.
- Yifan Li, Yifan Du, Kun Zhou, Jinpeng Wang, Wayne Xin Zhao, and Ji-Rong Wen. 2023b. Evaluating object hallucination in large vision-language models. *arXiv preprint arXiv:2305.10355*.
- Yunxin Li, Shenyan Jiang, Baotian Hu, Longyue Wang, Wanqi Zhong, Wenhan Luo, Lin Ma, and Min Zhang. 2025. Uni-moe: Scaling unified multimodal llms with mixture of experts. *IEEE Transactions on Pattern Analysis and Machine Intelligence*.
- Bin Lin, Zhenyu Tang, Yang Ye, Jiayi Cui, Bin Zhu, Peng Jin, Jinfa Huang, Junwu Zhang, Yatian Pang, Munan Ning, and 1 others. 2024. Moe-llava: Mixture of experts for large vision-language models. *arXiv preprint arXiv:2401.15947*.
- Aixin Liu, Bei Feng, Bing Xue, Bingxuan Wang, Bochao Wu, Chengda Lu, Chenggang Zhao, Chengqi Deng, Chenyu Zhang, Chong Ruan, and 1 others. 2024. Deepseek-v3 technical report. *arXiv preprint arXiv:2412.19437*.
- Fuxiao Liu, Kevin Lin, Linjie Li, Jianfeng Wang, Yaser Yacoob, and Lijuan Wang. 2023a. Aligning large multi-modal model with robust instruction tuning. *CoRR*.
- Haotian Liu, Chunyuan Li, Yuheng Li, and Yong Jae Lee. 2023b. Improved baselines with visual instruction tuning. *arXiv preprint arXiv:2310.03744*.
- Yuan Liu, Haodong Duan, Yuanhan Zhang, Bo Li, Songyang Zhang, Wangbo Zhao, Yike Yuan, Jiaqi Wang, Conghui He, Ziwei Liu, and 1 others. 2023c. Mmbench: Is your multi-modal model an all-around player? *arXiv preprint arXiv:2307.06281*.
- Ka Man Lo, Zeyu Huang, Zihan Qiu, Zili Wang, and Jie Fu. 2024. A closer look into mixture-of-experts in large language models. *arXiv preprint arXiv:2406.18219*.
- Jinqiang Long, Yanqi Dai, Guoxing Yang, Hongpeng Lin, Nanyi Fei, Yizhao Gao, and Zhiwu Lu. 2024. Awaker2. 5-vl: Stably scaling mllms with parameter-efficient mixture of experts. *arXiv preprint arXiv:2411.10669*.
- Pan Lu, Swaroop Mishra, Tony Xia, Liang Qiu, Kai-Wei Chang, Song-Chun Zhu, Oyvind Tafjord, Peter Clark, and Ashwin Kalyan. 2022. Learn to explain: Multimodal reasoning via thought chains for science question answering. In *The 36th Conference on Neural Information Processing Systems (NeurIPS)*.
- Gen Luo, Xue Yang, Wenhan Dou, Zhaokai Wang, Jiawen Liu, Jifeng Dai, Yu Qiao, and Xizhou Zhu. 2024. Mono-internvl: Pushing the boundaries of monolithic multimodal large language models with endogenous visual pre-training. *arXiv preprint arXiv:2410.08202*.
- Sheng Shen, Zhewei Yao, Chunyuan Li, Trevor Darrell, Kurt Keutzer, and Yuxiong He. 2023. Scaling vision-language models with sparse mixture of experts. *arXiv preprint arXiv:2303.07226*.
- Amanpreet Singh, Vivek Natarajan, Meet Shah, Yu Jiang, Xinlei Chen, Dhruv Batra, Devi Parikh, and Marcus Rohrbach. 2019. Towards vqa models that can read. In *Proceedings of the IEEE/CVF conference on computer vision and pattern recognition*, pages 8317–8326.
- Mirac Suzgun, Nathan Scales, Nathanael Schärli, Sebastian Gehrmann, Yi Tay, Hyung Won Chung, Aakanksha Chowdhery, Quoc V Le, Ed H Chi, Denny Zhou, and 1 others. 2022. Challenging big-bench tasks and whether chain-of-thought can solve them. *arXiv preprint arXiv:2210.09261*.
- Junke Wang, Lingchen Meng, Zejia Weng, Bo He, Zuxuan Wu, and Yu-Gang Jiang. 2023. To see is to believe: Prompting gpt-4v for better visual instruction tuning. *arXiv preprint arXiv:2311.07574*.
- Peng Wang, Shuai Bai, Sinan Tan, Shijie Wang, Zhihao Fan, Jinze Bai, Keqin Chen, Xuejing Liu, Jialin Wang, Wenbin Ge, and 1 others. 2024. Qwen2-vl: Enhancing vision-language model’s perception of the world at any resolution. *arXiv preprint arXiv:2409.12191*.
- Zhiyu Wu, Xiaokang Chen, Zizheng Pan, Xingchao Liu, Wen Liu, Damai Dai, Huazuo Gao, Yiyang Ma, Chengyue Wu, Bingxuan Wang, and 1 others. 2024. Deepseek-vl2: Mixture-of-experts vision-language models for advanced multimodal understanding. *arXiv preprint arXiv:2412.10302*.
- Weihao Yu, Zhengyuan Yang, Linjie Li, Jianfeng Wang, Kevin Lin, Zicheng Liu, Xinchao Wang, and Lijuan Wang. 2023. Mm-vet: Evaluating large multimodal models for integrated capabilities. *arXiv preprint arXiv:2308.02490*.
- Sukwon Yun, Inyoung Choi, Jie Peng, Yangfan Wu, Jinxuan Bao, Qiyiwen Zhang, Jiayi Xin, Qi Long, and Tianlong Chen. 2024. Flex-moe: Modeling arbitrary modality combination via the flexible mixture-of-experts. *arXiv preprint arXiv:2410.08245*.
- Bo Zhao, Boya Wu, and Tiejun Huang. 2023. Svit: Scaling up visual instruction tuning. *arXiv preprint arXiv:2307.04087*.

Jeffrey Zhou, Tianjian Lu, Swaroop Mishra, Sidhartha Brahma, Sujoy Basu, Yi Luan, Denny Zhou, and Le Hou. 2023. Instruction-following evaluation for large language models. *arXiv preprint arXiv:2311.07911*.

A Datasets and Training Details

As shown in Table 6, we merge the datasets used in stages 2 and 3 of MoE-LLaVA into a single training stage. The proportion of pure-text data in stage2 is only 2.5%.

Phase	Source	#Sample
Stage I	LLaVA-1.5-558k	558k
Stage II	SViT-157k,LVIS-220k,LRV-331k,MIMIC-IT-256k, LLaVA 1.5-mix-665k	1.6M

Table 6: Composition of the training datasets.

Hyper-parameter	Stage 1	Stage 2
batch size	128	256
learning rate	5e-4	2e-5
learning rate schedule	cosine	cosine
learning rate warm-up ratio	0.03	0.03
weight decay	0	0
grad norm clipping	1.0	1.0
epoch	1	1
optimizer	AdamW	AdamW
float precision	bfloat16	bfloat16
d_{min}, d_{max}	None	1.5, 2.0
α	None	0
β	None	0.01
deepspeed configuration	zero3	zero3

Table 7: Hyper-parameter for training.